HHS Public Access

Author manuscript

Proc SPIE Int Soc Opt Eng. Author manuscript; available in PMC 2016 May 17.

Published in final edited form as:

Proc SPIE Int Soc Opt Eng. 2016 March 21; 9784: . doi:10.1117/12.2216511.

Segmentation and labeling of the ventricular system in normal pressure hydrocephalus using patch-based tissue classification and multi-atlas labeling

Lotta M. Ellingsen[a,b], **Snehashis Roy**[c], **Aaron Carass**[b], **Ari M. Blitz**[d], **Dzung L. Pham**[c], and **Jerry L. Prince**[b]

[a]Department of Electrical and Computer Engineering, University of Iceland, Reykjavik, Iceland [b]Department of Electrical and Computer Engineering, The Johns Hopkins University, Baltimore, MD 21218, USA [c]CNRM, The Henry M. Jackson Foundation for the Advancement of Military Medicine, Bethesda, MD 20892, USA [d]Department of Radiology and Radiological Science, Johns Hopkins University, Baltimore, MD 21287, USA

Abstract

Normal pressure hydrocephalus (NPH) affects older adults and is thought to be caused by obstruction of the normal flow of cerebrospinal fluid (CSF). NPH typically presents with cognitive impairment, gait dysfunction, and urinary incontinence, and may account for more than five percent of all cases of dementia. Unlike most other causes of dementia, NPH can potentially be treated and the neurological dysfunction reversed by shunt surgery or endoscopic third ventriculostomy (ETV), which drain excess CSF. However, a major diagnostic challenge remains to robustly identify shunt-responsive NPH patients from patients with enlarged ventricles due to other neurodegenerative diseases. Currently, radiologists grade the severity of NPH by detailed examination and measurement of the ventricles based on stacks of 2D magnetic resonance images (MRIs). Here we propose a new method to automatically segment and label different compartments of the ventricles in NPH patients from MRIs. While this task has been achieved in healthy subjects, the ventricles in NPH are both enlarged and deformed, causing current algorithms to fail. Here we combine a patch-based tissue classification method with a registration-based multi-atlas labeling method to generate a novel algorithm that labels the lateral, third, and fourth ventricles in subjects with ventriculomegaly. The method is also applicable to other neurodegenerative diseases such as Alzheimer's disease; a condition considered in the differential diagnosis of NPH. Comparison with state of the art segmentation techniques demonstrate substantial improvements in labeling the enlarged ventricles, indicating that this strategy may be a viable option for the diagnosis and characterization of NPH.

Keywords

MRI; enlarged brain ventricles; segmentation; labeling; hydrocephalus

Further author information: (Send correspondence to L.M.E.), L.M.E.: lotta@jhu.edu, J.L.P.: prince@jhu.edu.

1. INTRODUCTION

The ventricular system of the human brain consists of four main cavities, two large lateral ventricles and the third and fourth ventricles (see Fig. 1A). All four ventricles contain a network of blood vessels, called choroid plexus, that produces CSF. The CSF flows through the ventricular space within the brain, bathes the entire central nervous system, and eventually reaches the venous system. The entire volume of CSF is renewed two to three times per day.[1] Disruption of flow can lead to excess CSF and a clinical condition called hydrocephalus. If this happens on a chronic basis it is classified as the clinical syndrome of normal pressure hydrocephalus (NPH), which is most common in the elderly. In NPH, the ventricles expand and press against nearby brain tissue causing the brain shape to become distorted, which can lead to brain damage (see Fig. 1B).

NPH typically presents with cognitive impairment, gait dysfunction, and urinary incontinence, and may account for more than five percent of all cases of dementia (U.S. News & World Report on Health, February, 2015). However, unlike other well-known causes of dementia, such as Alzheimer's disease (AD), once diagnosed, NPH patients have the option of shunt surgery or endoscopic third ventriculostomy (ETV) making NPH a potentially reversible cause of dementia. Given this potential therapeutic option it is important to diagnose those patients who will respond well to ETV or shunt surgery.[2] However, the diagnosis remains challenging since there are no distinctive pathognomonic features for NPH,[2–4] and it has even been suggested that the definitive diagnosis of this condition should be based on patient's response to the surgery itself.[5] At present, NPH is diagnosed by physical examination (gait evaluation) and brain imaging and the likelihood of positive response to therapy is determined using a lumbar puncture.[5] Patients who show clinical improvement (as measured by improvement in gait) following a lumbar puncture are candidates for shunt placement[6] or ETV. The lumbar puncture procedure, however, is not without risks[7] and a negative lumbar puncture test has a very low predictive accuracy.[2, 8] Therefore, a major diagnostic challenge remains to identify patients with NPH, and in particular, those who are likely to benefit from ETV or shunt surgery. This paper proposes an automatic method to analyze the ventricular structure in MR images so that the derived quantitative measures might help to address this challenge.

MR images from individuals suffering from NPH often show disproportionate dilatation of the compartments proximal to the region of CSF flow restriction and relative compression of those distal to the same site. An automatic segmentation and labeling method for the ventricular system could therefore be of great clinical value[9, 10] enabling quantification of the relative size of the different ventricular compartments. Such a tool could give clues of where the location of obstruction is and in turn help distinguish shunt responsive vs. non-responsive NPH patients and help in surgical planning. Such a methodology could also allow researchers to subgroup cases of NPH to elucidate individual causes. However, segmenting the ventricles in NPH patients is challenging given their massively enlarged and distorted ventricles.

The ventricular system is routinely segmented as a single unit using MRI by several algorithms and their associated software packages. Among those freely available are

FIRST,[11] SPM,[12] TOADS,[13] and volBrain.[14] A key limitation of all of these methods is their inability to parcellate the ventricular system into multiple compartments in order to compute volumetric ratios within the ventricles. Segmentation and labeling of the ventricular system into its four main compartments, however, has been carried out by several multi-atlas label fusion approaches.[15–17] Multi-atlas label fusion methods have been shown to outperform other methods in segmenting multiple sub-cortical structures, both on normal and several diseased populations.[18] However, NPH patients have not been included in any of these evaluations, limiting the value of these evaluations, since the enlarged ventricles in NPH patients tend to cause significant segmentation errors. Our own experiments on NPH subjects have shown that state of the art registration based segmentation methods fail to correctly label the enlarged ventricles because the registration is unable to capture the severe anatomical shape and size differences between the atlas and the NPH subject (see results in Section 3). Previous methods designed specifically to handle NPH[19] cannot provide parcellations of the individual sub-components of the ventricular system. In this paper we present a novel image analysis method designed to take advantage of both tissue classification as well as multi-atlas segmentation to solve this difficult parcellation task by automatic image processing. The method is capable of segmenting and labeling individual compartments within the greatly enlarged ventricles in patients with NPH. The key innovation of our approach is the integration of two approaches, one for segmentation (S3DL[20]) and one for labeling (MALP-EM[17]), which together provide robustness and capabilities that neither possesses by itself. The availability of such an algorithm could dramatically stimulate research on a potentially treatable cause of dementia.

2. METHOD

The method presented integrates two segmentation approaches, i.e., the subject specific sparse dictionary learning (S3DL) method[20, 21] and the multi-atlas label propagation with expectation-maximization (MALP-EM) method.[17] S3DL is a patch-based tissue classification method that uses a sparse dictionary learning approach.[22] S3DL gives us classification results comprising seven labels that we partly incorporate into MALP-EM, a method that performs label fusion of multiple atlases, each with 138 labels, which have been registered to the subject. The key feature of MALP-EM is a special relaxation scheme that corrects the anatomical atlas priors in regions where accurate registration of the images is unachievable due to missing brain tissue or massive deformation. We use the S3DL labels in the relaxation scheme of MALP-EM, creating a novel method referred to as the RobUst DictiOnary-learning and Label Propagation Hybrid (RUDOLPH), that provides 1) a robust segmentation of the ventricular system and 2) an automatic parcellation of the ventricles into four compartments, i.e., lateral (left and right), third, and fourth ventricles in patients with enlarged ventricles. We chose this approach over using multiple NPH atlases in a multi-atlas label fusion method for the following two reasons: 1) the variability in the shape and size of ventricle enlargement in NPH is high and therefore would require a large number of atlases to capture the variability and substantially increase the processing time; and 2) manually labeled NPH subjects do not exist at this point and would take experts a significant amount of work to achieve.

The first step of RUDOLPH (as in MALP-EM) is to register 10 manually labeled atlases into the subject's space, each comprising 138 cortical and subcortical labels from the Neuromorphometrics dataset (see http://neuromorphometrics.com). For this process we use the SyN deformable registration method.[23] The output of this process is a probabilistic segmentation $\Pi = \{\pi_1, \pi_2, \ldots, \pi_n\}$, where π_i, $i = 1,\ldots, n$, (n is the total number of voxels) represent K-dimensional vectors with the kth component representing the probability that a voxel i belongs to the label k. Simultaneously, the MR image is processed with the S3DL[20] method. In addition to the MR image, S3DL requires one training data set (called an atlas), which comprises an MR image, its hard segmentation, and spatial priors depicting where different tissues are expected to be located. These priors can be computed using a variety of approaches but practically, a simple blurring of the known atlas segmentation suffices. S3DL adaptively modifies the subject priors to account for the potential high variability in the anatomical size and shape enabling robust segmentation of the ventricular system in patients with highly enlarged ventricles. The output of S3DL is the segmentation of the MR image into seven tissue classes: cerebral and cerebellar white matter, cortical, sub-cortical, and cerebellar gray matter, and cortical and ventricular CSF.

The S3DL labels for CSF are subsequently incorporated into our implementation of the registration-based multi-atlas label fusion method, MALP-EM,[17] where we have made critical changes to the algorithm to account for the added information from S3DL. MALP-EM provides two key label correction schemes: 1) it computes intensity-refined posterior probabilities and 2) it provides a relaxation framework to correct the anatomical atlas priors Π in regions where accurate registration of the images is unachievable due to severe deformation. MALP-EM was specifically designed to segment brain images expected to have severe changes in anatomical structure due to traumatic brain injury. Despite this, MALP-EM by itself fails to correctly label the ventricles of NPH patients, in part due to the close spatial proximity of ventricular and external CSF (red arrows in Fig. 1B). The proposed method, RUDOLPH, addresses this failure by incorporating the robust segmentation from S3DL into the relaxation scheme.

Assuming a Gaussian distribution, a common parameter set ($\mu_{\text{CSF-like}}$, $\sigma_{\text{CSF-like}}$) of eight CSF-like structures is estimated based on the probabilistic prior segmentation Π (including labels for external and sulcal CSF, and the 3rd, 4th, right/left inferior, and right/left lateral ventricles). For each structure k an individual parameter set (μ_k, σ_k) is also estimated based on Π. The probabilistic segmentation Π is then relaxed to Π^R based on image intensities in an attempt to correct inaccurate labels from the registration based segmentation. In the relaxation step in MALP-EM a fraction α_{ik} of the prior probability, π_{ik}, is redistributed from a structure k to one of the eight CSF-like structures k_{CSF}, where at an image voxel i, k_{CSF} is determined as the CSF-like structure with the highest prior probability or the CSF-like label that is spatially closest to the voxel. This is where MALP-EM fails when labeling the ventricles of NPH subjects. When a voxel is located at the boundary of an enlarged ventricle, the prior segmentation Π is incorrect due to the inability of the registration process to align the atlas ventricles to the enlarged NPH ventricles and the closest CSF-like structure is in the subarachnoid space (i.e., external CSF) and not the ventricle. Hence, the ventricle gets incorrectly labeled as external CSF (red labels in MALP-EM results in Fig. 2, third row). In RUDOLPH, instead of looking at the probabilistic prior segmentation Π from MALP-EM to

determine the closest CSF-like structure, we look at the segmentation from S3DL and determine k_{CSF} as:

$$k_{\mathrm{CSF}} = \begin{cases} \underset{k \text{ is CSF-like}}{\arg\max}\ \pi_{ik} & \text{if } \pi_{ik} \neq 0 \text{ for at least one } k \in \mathrm{CSF-like} \\ \underset{k \text{ is CSF-like in S3DL}}{\arg\min}\ d(k,i) & \text{otherwise} \end{cases}, \quad (1)$$

where $d(k, i)$ denotes the Euclidean distance of voxel i to the closest point in label k. The fraction α_{ik} is then calculated as in MALP-EM based on the probability that the voxel with intensity y_i comes either from the intensity distribution $\mathcal{N}_k^{\pi}$ estimated in label k or $\mathcal{N}_{\mathrm{CSF-like}}^{\pi}$, i.e.

$$\alpha_{ik} = \begin{cases} 0 & \text{if } \mathcal{N}_k^{\pi}(y_i) \geq \mathcal{N}_{\mathrm{CSF-like}}^{\pi}(y_i) \\ \max(0, \min(0.5 - \pi_{ik_{\mathrm{CSF}}}, \pi_{ik})) & \text{otherwise} \end{cases}. \quad (2)$$

The relaxed prior probability Π^R is calculated as in MALP-EM, where

$$\pi_{ik}^R = \begin{cases} \pi_{ik} + \sum_{l \neq k_{\mathrm{CSF}}} \alpha_{il} & \text{if } k = k_{\mathrm{CSF}} \\ \pi_{ik} - \alpha_{ik} & \text{otherwise} \end{cases}. \quad (3)$$

The improved priors Π^R are in turn refined in an intensity based EM framework and finally, the fusion based (i.e., Π) and EM-based segmentations are merged through a weighting scheme to generate the final segmentation, as in MALP-EM.

3. RESULTS

We processed a total of 14 NPH subjects using RUDOLPH and two state of the art segmentation and labeling methods: Freesurfer[24] and MALP-EM. Visual comparison (Fig. 2) of the three methods demonstrate more robust segmentation and labeling when using RUDOLPH, particularly on the more severe cases of NPH where both Freesurfer and MALP-EM fail dramatically (see subjects 11–14 in Fig. 2). Note that Freesurfer was run with the “bigventricles” switch to account for the enlarged ventricles. In order to quantitatively validate our method we manually labeled the ventricular system in all the subjects as one mask, including the lateral, third, and fourth ventricles. We computed the Dice coefficient between the automatically generated mask (combining all ventricular labels in one binary mask) and the manual labels to quantitatively evaluate their overlap. The Dice coefficient is significantly higher ($p < 0.05$) in RUDOLPH (Fig. 3, green bars) than Freesurfer (Fig. 3, blue bars) and substantially higher than MALP-EM (Fig. 3, red bars), particularly in subjects with greatly enlarged ventricles (see Fig. 3, right side). From the figure we can see that the Dice coefficient of RUDOLPH is quite stable for all subjects while the Dice coefficient for both MALP-EM and Freesurfer decreases with increasing ventricle size. The mean Dice coefficient for all 14 subjects was 0.72 for Freesurfer, 0.90 for MALP-EM, and 0.93 for RUDOLPH, with the Dice measure being comparable for all three methods when labeling subjects with only moderately enlarged ventricles (Fig. 2, left side). Further validation of the method will be carried out in the future, including a manual

labeling of the different compartments of the ventricular system to provide more detailed ground truth information.

4. CONCLUSIONS

A new method for segmenting and labeling the ventricular system of NPH patients is presented. The new method, RUDOLPH, integrates a patch-based tissue classification method (S3DL) with a registration-based multi-atlas labeling method (MALP-EM) providing a robust segmentation and labeling of the lateral (left and right), third, and fourth ventricles of the brain. Quantitative evaluation was carried out on 14 NPH subjects and the performance of RUDOLPH compared with two state of the art methods, demonstrating substantially improved segmentation and labeling in terms of overlap measure using the Dice coefficient. The most critical improvements were observed in the severe cases of NPH, where both Freesurfer and MALP-EM fail to capture the greatly enlarged ventricles. The automated method presented will therefore enable more extensive scientific studies of volumetric ratios within the ventricular system and provide tools that can be used in clinical evaluation and classification of NPH patients. Such a tool will also provide researchers with the means to study ventriculomegaly in other neurodegenerative diseases, such as Alzheimer's disease, as well as in normal aging.

REFERENCES

1. Nolte, J. The Human Brain: An Introduction to Its Functional Anatomy. Mosby/Elsevier; 2009.
2. Stein SC, Burnett MG, Sonnad SS. Shunts in normal-pressure hydrocephalus: do we place too many or too few? J. Neurosurg. 2006 Dec.105:815–822. [PubMed: 17405250]
3. Panagiotopoulos V, Konstantinou D, Kalogeropoulos A, Maraziotis T. The predictive value of external continuous lumbar drainage, with cerebrospinal fluid outflow controlled by medium pressure valve, in normal pressure hydrocephalus. Acta Neurochir (Wien). 2005 Sep.147:953–958. [PubMed: 16041469]
4. Leinonen V, Koivisto AM, Alafuzoff I, Pyykko OT, Rummukainen J, von Und Zu Fraunberg M, Jaaskelainen JE, Soininen H, Rinne J, Savolainen S. Cortical brain biopsy in long-term prognostication of 468 patients with possible normal pressure hydrocephalus. Neurodegener Dis. 2012; 10(1–4):166–169. [PubMed: 22343771]
5. Mori E, Ishikawa M, Kato T, Kazui H, Miyake H, Miyajima M, Nakajima M, Hashimoto M, Kuriyama N, Tokuda T, Ishii K, Kaijima M, Hirata Y, Saito M, Arai H. Guidelines for management of idiopathic normal pressure hydrocephalus: second edition. Neurol. Med. Chir. (Tokyo). 2012; 52(11):775–809. [PubMed: 23183074]
6. Kang K, Ko PW, Jin M, Suk K, Lee HW. Idiopathic normal-pressure hydrocephalus, cerebrospinal fluid biomarkers, and the cerebrospinal fluid tap test. J Clin Neurosci. 2014 Aug.21:1398–1403. [PubMed: 24836892]
7. Kaya D, Soysal P, Isik AT. Intracranial hypotension-like syndrome after a spinal tap test performed for idiopathic normal pressure hydrocephalus. Am J Alzheimers Dis Other Demen. 2015 Sep. 30:569–572. [PubMed: 25762438]
8. Shprecher D, Schwalb J, Kurlan R. Normal pressure hydrocephalus: diagnosis and treatment. Curr Neurol Neurosci Rep. 2008 Sep.8:371–376. [PubMed: 18713572]
9. Serulle Y, Rusinek H, Kirov II, Milch H, Fieremans E, Baxter AB, McMenamy J, Jain R, Wisoff J, Golomb J, Gonen O, George AE. Differentiating shunt-responsive normal pressure hydrocephalus from Alzheimer disease and normal aging: pilot study using automated MRI brain tissue segmentation. J. Neurol. 2014 Oct.261:1994–2002. [PubMed: 25082631]

10. Heckemann RA, Hammers A, Rueckert D, Aviv RI, Harvey CJ, Hajnal JV. Automatic volumetry on MR brain images can support diagnostic decision making. BMC Med Imaging. 2008; 8:9. [PubMed: 18500985]
11. Patenaude B, Smith SM, Kennedy DN, Jenkinson M. A bayesian model of shape and appearance for subcortical brain segmentation. NeuroImage. 2011; 56(3):907–922. [PubMed: 21352927]
12. Statistical parametric mapping (SPM). http://www.fil.ion.ucl.ac.uk/spm/.
13. Bazin PL, Pham DL. Topology-preserving tissue classification of magnetic resonance brain images. IEEE Trans Med Imaging. 2007 Apr.26:487–496. [PubMed: 17427736]
14. Coupe P, Manjon JV, Fonov V, Pruessner J, Robles M, Collins DL. Patch-based segmentation using expert priors: application to hippocampus and ventricle segmentation. Neuroimage. 2011 Jan. 54:940–954. [PubMed: 20851199]
15. Heckemann RA, Hajnal JV, Aljabar P, Rueckert D, Hammers A. Automatic anatomical brain MRI segmentation combining label propagation and decision fusion. Neuroimage. 2006 Oct.33:115–126. [PubMed: 16860573]
16. Rohlfing T, Russakoff DB, Maurer CR. Performance-based classifier combination in atlas-based image segmentation using expectation-maximization parameter estimation. IEEE Trans Med Imaging. 2004 Aug.23:983–994. [PubMed: 15338732]
17. Ledig C, Heckemann RA, Hammers A, Lopez JC, Newcombe VF, Makropoulos A, Lotjonen J, Menon DK, Rueckert D. Robust whole-brain segmentation: application to traumatic brain injury. Med Image Anal. 2015 Apr.21:40–58. [PubMed: 25596765]
18. Babalola KO, Patenaude B, Aljabar P, Schnabel J, Kennedy D, Crum W, Smith S, Cootes T, Jenkinson M, Rueckert D. An evaluation of four automatic methods of segmenting the subcortical structures in the brain. Neuroimage. 2009 Oct.47:1435–1447. [PubMed: 19463960]
19. Shiee N, Bazin PL, Cuzzocreo JL, Blitz A, Pham DL. Segmentation of brain images using adaptive atlases with application to ventriculomegaly. Inf Process Med Imaging. 2011; 22:1–12. [PubMed: 21761641]
20. Roy S, He Q, Sweeney E, Carass A, Reich DS, Prince JL, Pham DL. Subject-Specific Sparse Dictionary Learning for Atlas-Based Brain MRI Segmentation. IEEE J Biomed Health Inform. 2015 Sep.19:1598–1609. [PubMed: 26340685]
21. Roy S, Carass A, Prince JL, Pham DL. Subject Specific Sparse Dictionary Learning for Atlas based Brain MRI Segmentation. Mach Learn Med Imaging. 2014; 8679:248–255. [PubMed: 25383394]
22. Roy, S.; Jog, A.; Carass, A.; Prince, JL. Atlas based intensity transformation of brain MR images. In: Shen, L.; Liu, T.; Yap, P-T.; Huang, H.; Shen, D.; Westin, C-F., editors. [MBIA], Lecture Notes in Computer Science. Vol. 8159. Springer; 2013. p. 51-62.
23. Avants BB, Epstein CL, Grossman M, Gee JC. Symmetric diffeomorphic image registration with cross-correlation: evaluating automated labeling of elderly and neurodegenerative brain. Med Image Anal. 2008 Feb.12:26–41. [PubMed: 17659998]
24. Dale A, Fischl B, Sereno MI. Cortical surface-based analysis: I. segmentation and surface reconstruction. NeuroImage. 1999; 9(2):179–194. [PubMed: 9931268]

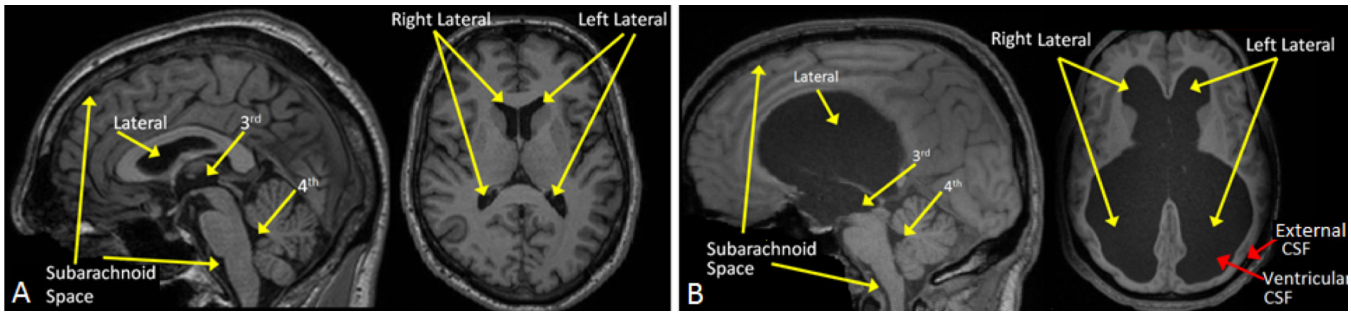

Figure 1.
MR images of the ventricular systems of A) a healthy subject and B) an NPH subject.

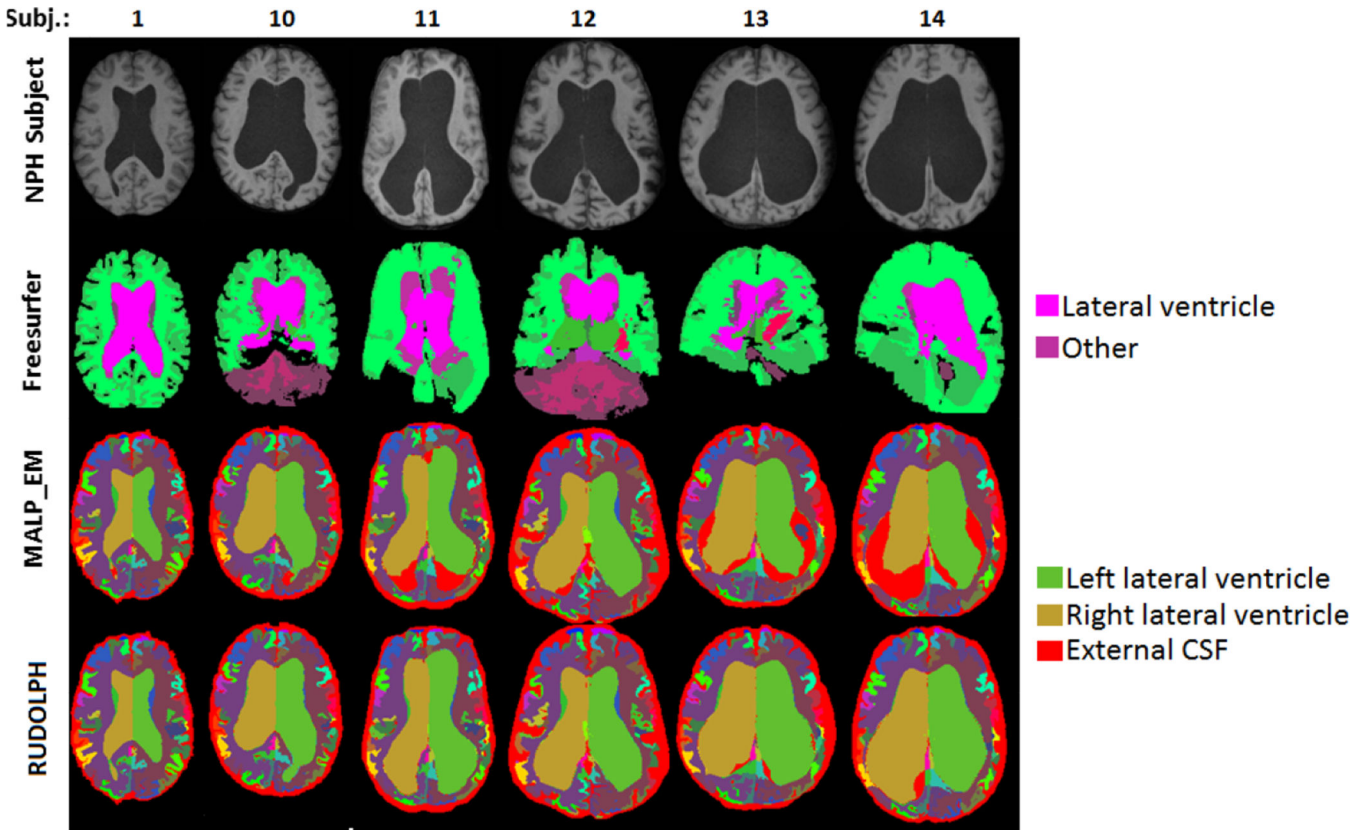

Figure 2.
NPH subjects (top row), Freesurfer (second row), MALP-EM (third row), and RUDOLPH (bottom row).

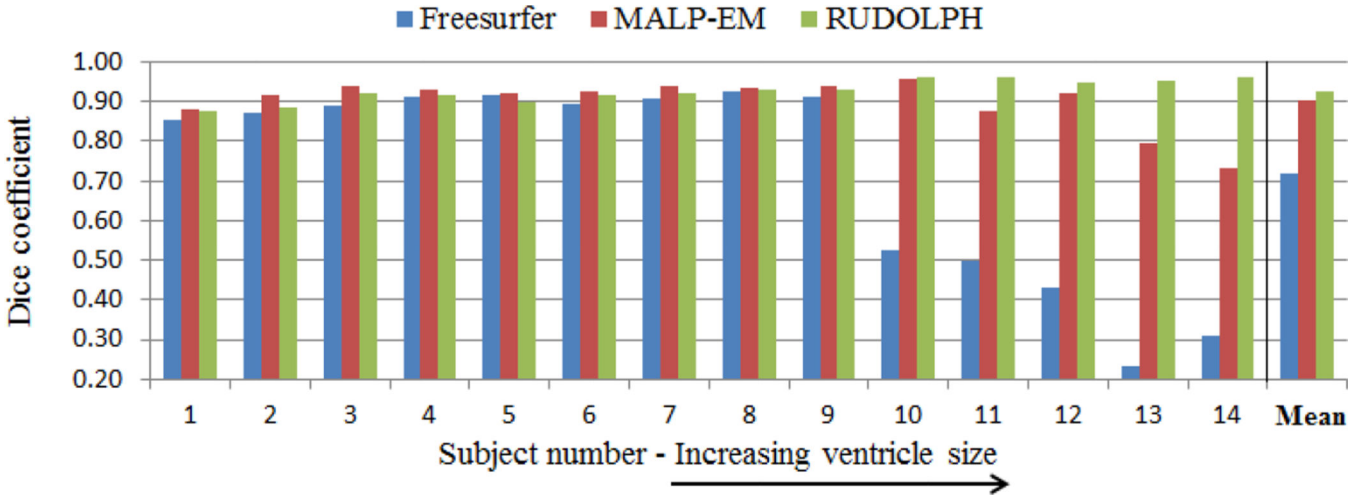

Figure 3.

Dice coefficient of the overlap between the automatically and manually labeled ventricular system for Freesurfer (blue), MALP-EM (red) and RUDOLPH (green). The subjects are ordered left to right according to their ventricle size from the smallest to the largest.